

11. Jamieson, I. G. & Craig, J. L. Male-male and female-female courtship and copulation behaviour in a communally breeding bird. *Anim. Behav.* **35**, 1251-1253 (1987).
12. Hamilton, W. D. The genetical evolution of social behaviour. *J. Theor. Biol.* **7**, 1-16 (1964).
13. Ens, B. J. Guarding your mate and losing the egg: an oystercatcher's dilemma. *Wader Study Group Bull.* **61**, 69-70 (1991).
14. Drent, R. in *Avian Biology*, Vol. 5 (eds Farner, D. S. & King, J. R.) 333-420 (Academic, New York, 1975).
15. Webb, D. R. Thermal tolerance of avian embryos: a review. *Condor* **89**, 874-898 (1987).
16. Ens, B. J., Kersten, M., Breninkmeijer, A. & Hulscher, J. B. Territory quality, parental effort and reproductive success of oystercatchers (*Haematopus ostralegus*). *J. Anim. Ecol.* **61**, 703-715 (1992).
17. Ens, B. J., Weissing, F. J. & Drent, R. H. The despotic distribution and deferred maturity: two sides of the same coin. *Am. Nat.* **146**, 625-650 (1995).
18. Queller, D. C. & Goodnight, K. F. Estimating relatedness using genetic markers. *Evolution* **43**, 258-275 (1989).
19. Blouin, M. S., Parsons, M., Lacaille, V. & Lotz, S. Use of microsatellite loci to classify individuals by relatedness. *Mol. Ecol.* **5**, 393-401 (1996).

Acknowledgements. D.H. was supported by a grant and R.v.T. by a fellowship from the Netherlands Organization for Scientific Research. We thank B. J. Ens, L. van de Zande, M. Kersten, J. B. Hulscher, A. Breninkmeijer, K. van Oers, I. de Groot, A. Helmhout, L. Klösters, R. Krijnen, F.-J. Voogd and N. J. Dingemans for participating in the project; J. Koenes, J. Nijboer, W. Beukema and D. Visser for technical assistance; Natuurmonumenten for permission to work in their reserve; and R. H. Drent, B. J. Ens, J. B. Hulscher, J. Tinbergen and J. P. Kruijff for suggestions. The Animal Experiments Committee RuG gave permission for blood sampling and temporary clutch manipulations.

Correspondence and requests for materials should be addressed to D.H. (e-mail: d.h.heg@biol.rug.nl).

Evidence for evolutionary conservation of sex-determining genes

Christopher S. Raymond*, Caroline E. Shamu†‡, Michael M. Shen†‡, Kelly J. Seifert§, Betsy Hirsch§, Jonathan Hodgkin† & David Zarkower*

* Institute of Human Genetics and Department of Biochemistry and § Department of Laboratory Medicine and Pathology, University of Minnesota Medical School, Minneapolis, Minnesota 55455, USA

† MRC Laboratory of Molecular Biology, Hills Road, Cambridge CB2 2QH, UK

Most metazoans occur as two sexes. Surprisingly, molecular analyses have hitherto indicated that sex-determining mechanisms differ completely between phyla. Here we present evidence to the contrary. We have isolated the male sexual regulatory gene *mab-3* (ref. 1) from the nematode *Caenorhabditis elegans* and found that it is related to the *Drosophila melanogaster* sexual regulatory gene *doublesex* (*dsx*)². Both genes encode proteins with a DNA-binding motif³ that we have named the 'DM domain'. Both genes control sex-specific neuroblast differentiation and yolk protein gene transcription; *dsx* controls other sexually dimorphic features as well. The form of DSX that is found in males can direct male-specific neuroblast differentiation in *C. elegans*. This structural and functional similarity between phyla suggests a common evolutionary origin of at least some aspects of sexual regulation. We have identified a human gene, *DMT1*, that encodes a protein with a DM domain and find that *DMT1* is expressed only in testis. *DMT1* maps to the distal short arm of chromosome 9, a location implicated in human XY sex reversal⁴. Proteins with DM domains may therefore also regulate sexual development in mammals.

Sexual development in *C. elegans* is controlled by a series of global regulatory genes⁶. The terminal global regulator, *tra-1*, acts as a genetic switch that can direct all aspects of somatic sexual development^{7,8} and which is also important in germline sexual development^{8,9}. Thus, *tra-1* must control, directly or indirectly, most sex-specific genes. The *tra-1* gene probably acts through several downstream regulators, each of which controls more

restricted aspects of sexual development. An analogous situation is found in *Drosophila*, where a different pathway of global regulators sets the activity of downstream genes that include *dsx*², *fruitless*^{10,11} and *dissatisfaction*¹². Despite the widespread occurrence of sexual dimorphism across phyla, until now no sexual regulatory genes have been found to be related between distant species.

The *mab-3* gene acts downstream of *tra-1* to promote male-specific development of two tissues¹. In the peripheral nervous system, *mab-3* activity directs differentiation of sensory ray neuroblasts into peripheral sense organs (V rays). In the intestine, *mab-3* plays an entirely different role, causing repression of vitellogenin (yolk protein) gene transcription.

We mapped the location of the *mab-3* gene by determining the

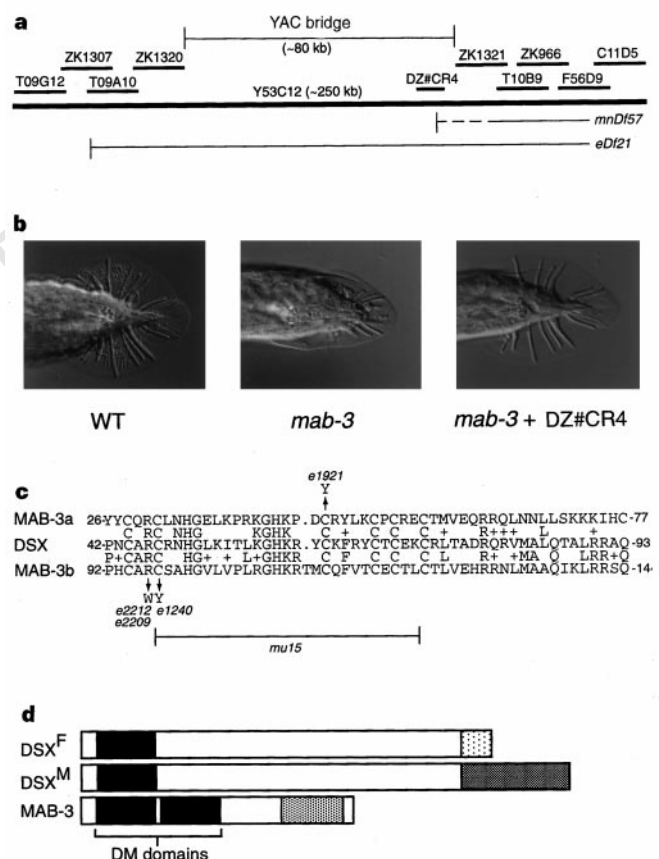


Figure 1 Isolation and characterization of the *mab-3* gene. **a**, Diagram of *mab-3* genomic region. Horizontal lines indicate positions of cosmids, phage clone DZ#CR4, and the yeast artificial chromosome clone Y53C12. *mab-3* lies between the endpoints of *eDf21* and *mnDf57*. **b**, Rescue of *mab-3* mutation by phage clone DZ#CR4. Ventral views of the tail are shown. A wild-type male tail is at the left; it has six V rays and three more posterior T rays on each side. The effect of mutant allele *e1240* is shown in the centre; T rays are present, but V rays are missing. Mutant transformed with phage clone (right) has 10 of 12 V rays restored. Nomarski optics; the original magnification was $\times 400$. **c**, Comparison of DSX and MAB-3 DM domains. Identical residues are shown in rows between protein sequences; similar residues indicated by plus signs. Amino-acid changes in *mab-3* mutants are indicated. MAB-3a is the first DM domain; MAB-3b is the second DM domain. The *mu15* allele lacks the indicated protein-coding region and most of the next intron. **d**, Diagrams of DSX and MAB-3 proteins. *dsx* is spliced to form mRNAs encoding sex-specific proteins² DSX^M and DSX^F. DM domains are indicated by filled boxes; sex-specific DSX domains and the C-terminal proline- and serine-rich region of MAB-3 are indicated by stippled boxes. The region of similarity in the DM domain corresponds closely to the minimal DNA-binding domain defined for DSX³.

‡ Present addresses: Department of Cell Biology, Harvard Medical School, Boston, Massachusetts 02115, USA (C.E.S.); Center for Advanced Biotechnology and Medicine, and Department of Pediatrics, UMDNJ-Robert Wood Johnson Medical School, 679 Hoes Lane, Piscataway, New Jersey 08854, USA (M.M.S.).

physical endpoints of genetic deficiencies (Fig. 1a). We isolated a phage clone, DZ#CR4, containing this gene. When microinjected into *mab-3* mutants, DNA from this phage clone rescues the *mab-3* mutant phenotype (Fig. 1b). We further narrowed the rescuing activity to a 7-kb interval by microinjecting DNA fragments derived from DZ#CR4 into *mab-3* mutants.

The minimal *mab-3* rescuing fragment encodes a protein with two copies of a motif similar to the DNA-binding domain of the *Drosophila* sexual regulator DSX (Fig. 1c). This domain chelates zinc and confers sequence-specific DNA binding, but is distinct from a classical zinc-finger^{3,13}. On the basis of its occurrence in DSX and MAB-3, we have named this motif the DM domain.

We sequenced DNA from the six existing *mab-3* mutant alleles and found mutations in all of them, confirming that this gene is *mab-3*. One allele, *e1921*, encodes a protein with a cysteine-to-tyrosine mutation of a conserved residue in the first DM domain (Fig. 1c), demonstrating that this domain is important for *mab-3* function. Four alleles are altered in the region encoding the second DM domain, demonstrating that this domain is also required. The canonical null allele *e1240* (refs 1, 14) encodes a protein with a cysteine-to-tyrosine mutation of a conserved residue in the second DM domain. In DSX, this cysteine is essential for DNA binding *in vitro* and for function *in vivo*³. A second null allele, *mu15*, contains a deletion that removes most of the second DM domain and the next splice junction. Two less severe loss-of-function alleles, *e2209* and *e2212*, encode proteins with the same arginine-to-tryptophan mutation. The sixth, and least severe, mutant, *e2093*, has a UAA (ochre) nonsense mutation near the 3' end, truncating the MAB-3 protein by 52 amino acids. As in DSX, the DM domains are near the amino terminus of MAB-3 (Fig. 1d).

Three mRNAs, which are formed by alternative splicing (Fig. 2a), are expressed from the *mab-3* locus. Reverse transcription with polymerase chain reaction (RT-PCR) experiments detected two *trans*-spliced messenger RNAs. The longer mRNA (~1.8 kb) encodes full-length MAB-3 protein with two DM domains. The shorter mRNA (~1.6 kb) starts just before the second DM domain. As the first AUG in this mRNA is found after the second DM domain, any protein it encodes would lack both domains. The third and shortest mRNA (~1.5 kb), identified as a cDNA clone (yk69b1; Y. Kohara, personal communication), incorporates an alternative exon with translational stops in all three frames. It may be non-functional, or it might encode a small peptide consisting of the carboxy terminus of MAB-3.

The *mab-3* mRNA is sex-specifically expressed (Fig. 2b). It is expressed in late larvae of both sexes, when *mab-3* mutations first affect the V neuroblasts¹. In the fourth larval stage, expression is approximately sixfold higher in males than in hermaphrodites. It is not clear whether the *mab-3* mRNA has a function in hermaphrodites, as *mab-3* mutations in hermaphrodites exhibit no detectable phenotype¹. In adults, expression of *mab-3* mRNA is undetectable in XX hermaphrodites, but persists in XO males. Activity of *tra-1* is required in XX animals to repress *mab-3* activity¹. Likewise, we find that *tra-1* activity is required to prevent accumulation of *mab-3* mRNA in XX animals (Fig. 2b). In adult *tra-1*(null) XX phenotypic males, *mab-3* mRNA accumulates to levels found in normal XO males.

The *mab-3* and *dsx* genes are similar not only in sequence but also in their roles in sexual development. Both genes control the differentiation of sex-specific neuroblasts into peripheral sense organs and regulate transcription of yolk protein genes. (Dipteran

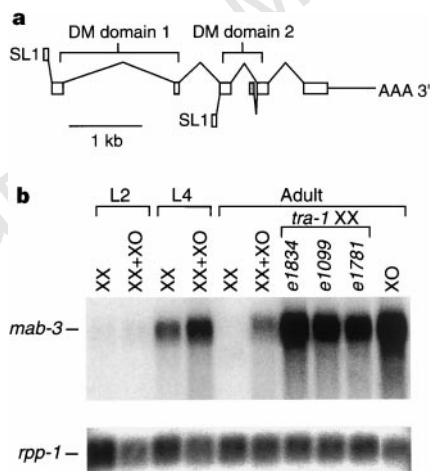


Figure 2 Splicing pattern and mRNA expression of *mab-3*. **a**, Splicing diagram. Exons are indicated by boxes and introns by lines. Spliced leader RNA SL1 is added by *trans*-splicing at positions indicated. The stippled exon contains stop codons in all three potential translational reading frames. **b**, RNA blot. Poly(A)⁺ mRNA from developmentally staged nematodes was separated by agarose gel electrophoresis and probed with a cDNA probe derived from exons 4 and 5, which are common to all three *mab-3* mRNAs. The predominant mRNAs detected are the full-length (~1.8 kb) and the shorter (~1.6 kb) *trans*-spliced mRNAs. The shortest mRNA (~1.5 kb) is not detected, is less abundant, and is not sex-specific. Chromosomal sex of animals is indicated: XX animals are wild-type hermaphrodites and XO animals are *him-8* males. XX + XO indicates mRNA from mixed sex *him-8* populations. XX *tra-1* animals are phenotypic males. The bottom panel shows a loading control in which the blot is reprobated with the *rp21* (*rpp-1*) ribosomal protein probe. L2 and L4, larval stages.

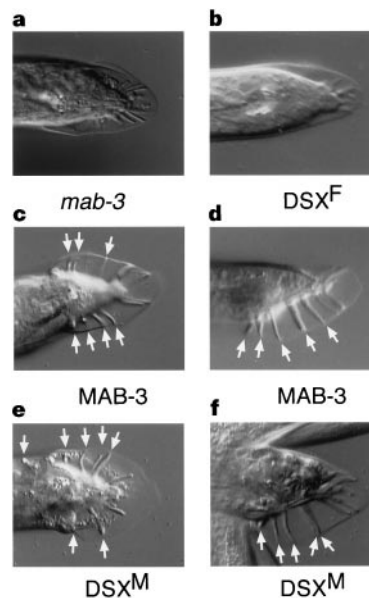


Figure 3 Male DSX, but not female DSX, can direct V-ray formation in *C. elegans*. **a**, *mab-3*(*e1240*) male with no transgene, ventral view. **b-f**, *mab-3*(*e1240*) males from transgenic strains were heatshocked. Transgenes encode DSX^F (**b**, ventral view), MAB-3 (**c**, ventral view and **d**, lateral view) or DSX^M (**e**, ventral view and **f**, ventral lateral view). V rays are indicated by white arrows. MAB-3 and DSX^M restore V rays, whereas DSX^F does not. In most animals the copulatory bursa is cupped, and it is usually not possible to photograph all rays in one focal plane. The percentages of V rays per side (wild-type animals have six rays, or 100%, per side) were as follows: *mab-3*(*e1240*) alone, 8% (240 sides counted); *e1240* expressing MAB-3 transgene, 32% (65 sides counted); *e1240* expressing DSX^M transgene, 35% (184 sides counted); *e1240* expressing DSX^F transgene, 5% (319 sides counted).

of sexual regulation arose before the divergence of Nematoda and Arthropoda and have been conserved. □

Methods

C. elegans strains and culture. Culture and genetic manipulation of *C. elegans* were performed as previously described²³. Phenotypically wild-type males carried the *him-8(e1489)* mutation, which causes high incidence (~40%) of males due to X-chromosome nondisjunction. *mab-3* mutants were genotype *mab-3(e1240); him-5(e1490)*. Transgenic nematodes were generated by standard methods²⁴, with the dominant transformation marker *rol-6(su1006)* at 100 ng μl^{-1} . XO males were isolated by filtration through nylon screens²³, yielding >95% pure XO males. *tra-1* mutant pseudomales were derived from strains of genotype *tra-1(lf); eDp6* (*eDp6* is a free duplication containing a wild-type *tra-1* gene). Spontaneous loss of *eDp6* leads to ~40% homozygous *tra-1(lf)* animals in the population²⁵. These XX phenotypic males were isolated by filtration.

DNA clones and libraries. The *C. elegans* ribosomal protein gene *rp21* (*rpp-1*) cDNA clone pPD33.24 was a gift from A. Fire. The *DMT1* cDNA clone (Genbank accession number AA412330) was purchased from Genome Systems (St Louis). The *mab-3* cDNA clone yk69b1 (Genbank accession number D65822) was a gift from Y. Kohara. Accession numbers for *C. elegans* DM-domain-containing genes are as follows: *mab-3* (AF022388), F10C1.5 (U49831), C34D1.1 (Z78060A), C34D1.2 (Z78060B), and F13G11.a (Z83317). The *M. scalaris* gene accession number is Y10341. Multiple sequence alignments were performed using the PIMA 1.4 (<http://dot.imgen.bcm.tmc.edu:9331/multi-align/multi-align.html>) and BOXSHADE 3.21 (http://ulrec3.unil.ch/software/BOX_form.html) programs.

Cloning of *mab-3*. We mapped the location of *mab-3* by determining the endpoints of genetic deficiencies (Fig. 1a). *mnDf57* (ref. 26), which does not remove *mab-3*, ends between cosmids ZK1321 and ZK1320, while *eDf21* (ref. 1), which does remove *mab-3*, ends in cosmid ZK1307. These deficiencies thus defined an uncloned region of ~80–100 kb containing *mab-3*. We made a plasmid library of *EcoRI* fragments from the overlying yeast artificial chromosome clone Y53C12 in pBluescript II. We sequenced random clones, and identified those that were neither yeast contaminants nor derived from the previously sequenced ends of Y53C12. Fragments were positioned relative to the ends of existing contigs by polymerase chain reaction (PCR) using the Expand Long polymerase (Boehringer). This identified one DNA fragment located 4 kb to the left of the ZK1321 contig. We probed a λ phage library from yeast carrying Y53C12 with this fragment, identifying five overlapping clones from 10,000 p.f.u. plated. We microinjected one clone, DZ#CR4, into *mab-3(e1240); him-5(e1490)* and found rescue of the *mab-3* phenotype both in F₁ progeny of injected animals and in four out of four transmitting lines carrying extrachromosomal arrays (Fig. 1b).

RT-PCR. Random-primed cDNA was made from RNA of mixed-sex L4 *him-8(e1489)* animals using the cDNA Cycle Kit (Invitrogen). To identify trans-spliced *mab-3* mRNAs, we performed reverse transcription (RT)-PCR with spliced leader SL1 and SL2 primers as described²⁷. Reverse *mab-3* primers were derived from exons 3, 4 and 5. PCR products were gel-purified and directly sequenced by [³³P]-labelled dideoxynucleotide (Amersham) cycle sequencing. This identified trans-splicing of SL1 to exons 1 and 3. One *mab-3* mRNA (represented by cDNA clone yk69b1) has an alternative exon with stop codons in all frames. RT-PCR and 5' RACE (rapid amplification of cDNA ends) PCR indicated that the alternative exon is the first exon in this splice variant. mRNA structures of the other two transcripts and full-length MAB-3 protein size were further confirmed by 5' RACE and by *in vitro* translation of *mab-3* cDNA.

Sequencing of *mab-3* alleles. Genomic DNA was isolated from six *mab-3* mutant strains as described²³. *mab-3* DNA was amplified by PCR, gel purified, and directly sequenced using [³³P]-labelled dideoxynucleotide (Amersham) cycle sequencing. The region encoding the second DM domain was sequenced from alleles *e1240*, *e2209*, *e2212* and *mu15*. Both DM domains were sequenced from alleles *e1921* and *e2093*. *e2093* is a double mutant, with a glutamine to asparagine mutation 3' to the UAA nonsense mutation.

RNA blotting. RNA isolation and blotting were performed as previously described²⁷, except that RNA was transferred to nylon membranes (Schleicher and Schuel) by pressure blotting. Blots were reprobed with an *rp21* cDNA probe as a loading control²⁸. The multiple human tissue blot was obtained from

Clontech (catalogue number 7770-01) and probed according to manufacturer's instructions². Tissues include ovary and uterus. Human poly(A)⁺ testis mRNA was purchased from Clontech. Tissue-blot hybridization was quantified using a Molecular Dynamics 445 SI phosphorimager and IPLab Gel software (Signal Analytics). As a control, the blot was probed for a ubiquitously expressed transcription factor, confirming that all spots contain intact mRNA.

Heatshock experiments. *mab-3*, *dsx^f* and *dsx^m* cDNAs were cloned into the heatshock vectors pPD49.78 and pPD49.83 (gifts from A. Fire) and co-injected into *mab-3(e1240); him-5(e1490)* hermaphrodites with pRF4, both at 0.1 mg ml⁻¹. Results shown in Fig. 3 are from pPD49.78 constructs. Animals with extrachromosomal transgene arrays were allowed to lay eggs for 12 h at 20 °C. Progeny were raised at 20 °C for 24 h and heatshocked for 60 min at 33 °C every 12 h until they reached adulthood. V-ray formation was scored by Nomarski microscopy. Six independent lines with each cDNA were tested. Composition of arrays was confirmed by PCR.

Fluorescence *in situ* hybridization (FISH) mapping. Metaphase cells from peripheral blood lymphocytes of karyotypically normal human males were prepared by standard cytogenetic methods. FISH²⁹ was performed using a 1.5 kb *DMT1* cDNA fragment labelled by nick translation with digoxigenin-11-dUTP (Boehringer). Cells were co-hybridized with the biotin-labelled chromosome-9 probe D9Z1 (Oncor) and counterstained with 4,6-diamidino-2-phenylindole (DAPI). Probes were detected with rhodamine-labelled anti-digoxigenin antibodies and fluorescein isothiocyanate (FITC)-avidin (Oncor). 40 metaphase cells were examined using a triple-pass (DAPI/FITC/rhodamine) filter and images were captured using CytoVision software (Applied Imaging). In all cells examined, hybridization was detected on the distal short arm of both chromosomes 9. No signal was detected on any other chromosome. On the basis of the very distal position of *DMT1*, it was assigned to band 9p24.3. FISH results were confirmed in three separate experiments. Data from the Mouse Genome Database (http://mgd.niaia.affrc.go.jp/bin/query_homology) were used to compare the locations of *DMT1* and *tda-1*.

Received 17 July; accepted 27 October 1997.

- Shen, M. M. & Hodgkin, J. *mab-3*, a gene required for sex-specific yolk protein expression and a male-specific lineage in *C. elegans*. *Cell* **54**, 1019–1031 (1988).
- Burtis, K. C. & Baker, B. S. *Drosophila* doublesex gene controls somatic sexual differentiation by producing alternatively spliced mRNAs encoding related sex-specific polypeptides. *Cell* **56**, 997–1010 (1989).
- Erdman, S. E. & Burtis, K. C. The *Drosophila* doublesex proteins share a novel zinc finger related DNA binding domain. *EMBO J.* **12**, 527–535 (1993).
- Vetina, R. *et al.* Deletions of distal 9p associated with 46, XY male to female sex reversal: definition of the breakpoints at 9p23.3-p24.1. *Genomics* **41**, 271–274 (1997).
- Eicher, E. M. *et al.* Sex-determining genes on mouse autosomes identified by linkage analysis of C57BL/6J-Y^{POS} sex reversal. *Nature Genet.* **14**, 206–209 (1996).
- Hodgkin, J. in *The Nematode Caenorhabditis elegans* (ed. Wood, W. B.) 243–279 (Cold Spring Harbor Laboratory Press, New York, 1988).
- Hodgkin, J. A. & Brenner, S. Mutations causing transformation of sexual phenotype in the nematode *Caenorhabditis elegans*. *Genetics* **86**, 275–287 (1977).
- Hodgkin, J. A genetic analysis of the sex-determining gene, *tra-1* in the nematode *Caenorhabditis elegans*. *Genes Dev.* **1**, 731–745 (1987).
- Schedl, T., Graham, P. L., Barton, M. K. & Kimble, J. Analysis of the role of *tra-1* in germline sex determination in the nematode *Caenorhabditis elegans*. *Genetics* **123**, 755–769 (1989).
- Ito, H. *et al.* Sexual orientation in *Drosophila* is altered by the *satori* mutation in the sex-determination gene *fruitless* that encodes a zinc finger protein with a BTB domain. *Proc. Natl Acad. Sci. USA* **93**, 9687–9692 (1996).
- Ryner, L. C. *et al.* Control of male sexual behavior and sexual orientation in *Drosophila* by the *fruitless* gene. *Cell* **87**, 1079–1089 (1996).
- Finley, K. D., Taylor, B. J., Milstein, M. & McKeown, M. *dissatisfaction*, a gene involved in sex-specific behavior and neural development of *Drosophila melanogaster*. *Proc. Natl Acad. Sci. USA* **94**, 913–918 (1997).
- Erdman, S. E., Chen, H.-J. & Burtis, K. C. Functional and genetic characterization of the oligomerization and DNA binding properties of the *Drosophila* Doublesex proteins. *Genetics* **144**, 1639–1652 (1996).
- Hodgkin, J. Male phenotypes and mating efficiency in *Caenorhabditis elegans*. *Genetics* **103**, 43–64 (1983).
- Spieth, J., Denison, K., Kirtland, S., Cane, J. & Blumenthal, T. The *Caenorhabditis elegans* vitellogenin genes: short sequence repeats in the promoter regions and homology to the vertebrate genes. *Nucleic Acids Res.* **13**, 5283–5295 (1985).
- Baker, B. S. & Ridge, K. A. Sex and the single cell. I. On the action of major loci affecting sex determination in *Drosophila melanogaster*. *Genetics* **94**, 383–423 (1980).
- Whitfield, L. S., Lovell-Badge, R. & Goodfellow, P. N. Rapid sequence evolution of the mammalian sex-determining gene *SRY*. *Nature* **364**, 713–715 (1993).
- Tucker, P. K. & Lundrigan, B. L. Rapid evolution of the sex determining locus in Old World mice and rats. *Nature* **364**, 715–717 (1993).
- Koopman, P., Gubbay, J., Vivian, N., Goodfellow, P. & Lovell, B. R. Male development of chromosomally female mice transgenic for *Sry*. *Nature* **351**, 117–121 (1991).
- Kuwabara, P. E. Interspecies comparison reveals evolution of control regions in the nematode sex-determining gene *tra-2*. *Genetics* **144**, 597–607 (1996).
- de Bono, M. & Hodgkin, J. Evolution of sex determination in *Caenorhabditis*: unusually high divergence of *tra-1* and its functional consequences. *Genetics* **144**, 587–595 (1996).
- Wilkins, A. S. Moving up the hierarchy: a hypothesis on the evolution of a genetic sex determination pathway. *BioEssays* **17**, 71–77 (1995).

23. Sulston, J. & Hodgkin, J. in *The Nematode Caenorhabditis elegans* (ed. Wood, W. W.) 587–606 (Cold Spring Harbor Laboratory Press, Cold Spring Harbor, New York, 1988).
24. Mello, C. C., Kramer, J. M., Stinchcomb, D. & Ambros, V. Efficient gene transfer in *C. elegans*: extrachromosomal maintenance and integration of transforming sequences. *EMBO J.* **10**, 3959–3970 (1991).
25. Hodgkin, J. More sex-determination mutants of *Caenorhabditis elegans*. *Genetics* **96**, 649–664 (1980).
26. Sigurdson, D. C., Spanier, G. J. & Herman, R. K. *Caenorhabditis elegans* deficiency mapping. *Genetics* **108**, 331–345 (1984).
27. Zarkower, D. & Hodgkin, J. Molecular analysis of the *C. elegans* sex-determining gene *tra-1*: a gene encoding two zinc finger proteins. *Cell* **70**, 237–249 (1992).
28. Spieth, J., Shim, Y. H., Lea, K., Conrad, R. & Blumenthal, T. *elt-1*, an embryonically expressed *Caenorhabditis elegans* gene homologous to the GATA transcription factor family. *Mol. Cell Biol.* **11**, 4651–4659 (1991).
29. Trask, B. in *Genome Analysis: a Laboratory Manual* (eds Birren, B., Green, E., Hieter, P. & Myers, R.) (Cold Spring Harbor Laboratory Press, Cold Spring Harbor, NY, in the press).
30. McDonald, M. T., Flejter, W., Sheldon, S., Putzi, M. J. & Gorski, J. L. XY sex reversal and gonadal dysgenesis due to 9p24 monosomy. *Am. J. Med. Gen.* **73**, 321–326 (1997).

Acknowledgements. We thank colleagues at the University of Minnesota and MRC-LMB for discussions; M. de Bono for microinjection of cosmids from the *mab-3* region and for discussion; K. Burtis for *dsx* cDNAs; A. Coulson, J. Sulston, S. Chisoe and the *C. elegans* Genome Sequencing Consortium for assistance with physical mapping and sequencing of the *mab-3* region; C. Kenyon, C. Hunter and D. Cowing for the *mab-3(mul5)* allele; Y. Kohara for a *mab-3* cDNA clone; M. Sanders for a human-tissue blot; E. Parker for technical support; and V. Bardwell, J. Heasman, H. Towle, B. Van Ness and C. Wylie for critical reading of the manuscript. Some of the work by M.M.S. was performed in the laboratory of I. Greenwald, whom we thank. This work was supported by grants from the Minnesota Medical Foundation, University of Minnesota Graduate School and the NIH to D.Z., by NSF predoctoral fellowships to C.E.S. and M.M.S., and by the MRC and the HHMI.

Correspondence and requests for materials should be addressed to D.Z. (e-mail: zarkower@gene.med.umn.edu). Genbank accession number of the *mab-3* genomic sequence is AF022388.

Three neural tubes in mouse embryos with mutations in the T-box gene *Tbx6*

Deborah L. Chapman & Virginia E. Papaioannou

Department of Genetics and Development, College of Physicians and Surgeons of Columbia University, 701 W. 168th Street, New York, New York 10032, USA

Somites, segmented mesodermal units of the vertebrate embryo, are the precursors of adult skeletal muscle, bone and cartilage¹. During embryogenesis, somite progenitor cells ingress through the primitive streak, move laterally to a paraxial position (alongside the body axis) and segment into epithelial somites². Little is known about how this paraxial mesoderm tissue is specified^{1,2}. We have previously described a mouse T-box gene, *Tbx6* (ref. 3), which codes for a putative DNA-binding protein^{4,5}. The embryonic pattern of expression of *Tbx6* in somite precursor cells suggests that this gene may be involved in the specification of paraxial mesoderm³. We now report the creation of a mutation in *Tbx6* that profoundly affects the differentiation of paraxial mesoderm. Irregular somites form in the neck region of mutant embryos, whereas more posterior paraxial tissue does not form somites but instead differentiates along a neural pathway, forming neural-tube-like structures that flank the axial neural tube. These paraxial tubes show dorsal/ventral patterning that is characteristic of the neural tube, and have differentiated motor neurons. These results indicate that *Tbx6* is needed for cells to choose between a mesodermal and a neuronal differentiation pathway during gastrulation; *Tbx6* is essential for the specification of posterior paraxial mesoderm, and in its absence cells destined to form posterior somites differentiate along a neuronal pathway.

We created a mutation in the mouse T-box gene *Tbx6* by deleting the initiating methionine and a portion of the T-box, which codes for the putative DNA-binding domain of the protein^{4,5}, using homologous recombination in embryonic stem (ES) cells (Fig. 1). Animals heterozygous for the mutant allele, *Tbx6^{tm1Pa}*, were viable and fertile and had no obvious abnormalities, but no homozygotes were detected among 94 offspring resulting from matings of heterozygotes. Dissection of embryos resulting from intercross matings (see Methods) revealed a class of morphologically distinct embryos, which were first evident at embryonic day of development

(e) 8.5. These embryos had elongated normally, but lacked trunk somites and had enlarged tail buds and kinked neural tubes (Fig. 2a). Vascular anomalies were observed, such as multiple haematomas in the spinal cord and tail bud and the lack of segmental arteries, although the extraembryonic vasculature, including the allantoic connection to the placenta, appeared normal. By e11.5, abnormal embryos were oedematous and one out of five was dead, as judged by the lack of a heartbeat. By e12.5, all mutant embryos were dead, presumably because of haemorrhaging of embryonic blood vessels. Genotyping of 149 embryos, aged between e9.5 and e13.5, from 19 matings of heterozygotes revealed that all the embryos with this phenotype (18%) were homozygous mutants whereas the normal embryos were heterozygous or wild type.

Histological abnormalities were first detected at e8.5 when 3 out of 25 somite-stage embryos displayed enlarged tail buds and abnormalities in somite formation. Although 5–7 cranial somites were present and were differentiating into sclerotome and dermamyotome, epithelial condensations with a continuous central lumen were observed in paraxial mesoderm in more caudal regions. At e9.5 and e10.5, nine putative mutants examined had a characteristic enlarged tail bud containing a mass of undifferentiated mesenchymal cells (Fig. 2b and d), with multiple rosettes of epithelializing tissue found lateral to the neural tube (Fig. 2e) where somites would be forming in normal embryos. These condensations had central lumina which coalesced more rostrally into a single central lumen (Fig. 2f and i), resulting in two paraxial tubes extending to the level of the forelimb bud, parallel to the axial neural tube (Fig. 2h). Although these tubes were closed along much of their length, there were irregularly spaced, ventral openings where the lumen was continuous with the coelom (Fig. 2g). Areas of vascular leakage and oedema were present (Fig. 2f).

Histologically, the paraxial tubes seemed very similar to neural epithelium, and no segmentation or somite differentiation was seen

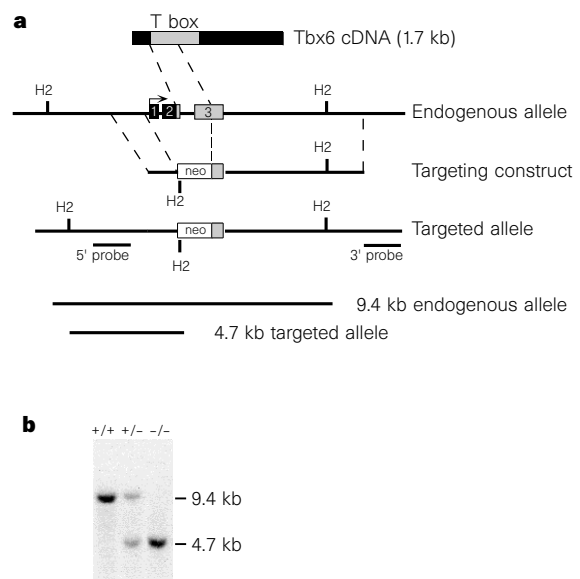


Figure 1 Targeted disruption of the *Tbx6* gene by homologous recombination. **a**, In the endogenous allele, the initiating methionine, is indicated by an arrow and the T-box, is stippled. The targeting-vector construct replaces the first two exons (1, 2) and a portion of the third exon (3) with the neomycin-resistance gene (*neo*), in reverse transcriptional orientation. Lines below the targeted allele and probes indicate the expected sizes for *HincII* (H2)-digested endogenous and targeted alleles detected by the 5'-external probe. The 3' external probe confirmed the targeting event. **b**, Southern-blot analysis of genomic DNA from embryos derived from matings between heterozygous mice. The 9.4-kilobase (kb) and 4.7-kb *HincII*-digested fragments corresponding to the wild-type (+) and targeted allele (-), respectively, were identified with the 5'-external probe shown in **a**.